Expected particle background

The sensitivity of our detectors will be significantly affected by the radiation environment. In particular, if we place our constellation to polar sun-synchronous orbits (SSO), we will experience increased background count rates around the polar regions due to the high flux of electrons. Therefore, a study of the expected particle background is especially important for designing the constellation and the trigger method.

The radiation belts around the Earth are the regions where energetic ions and electrons experience long-term magnetic trapping [1, 2]. Figure 1 shows the flux of trapped electrons with energy $E > 1$ MeV at altitude 500 km.

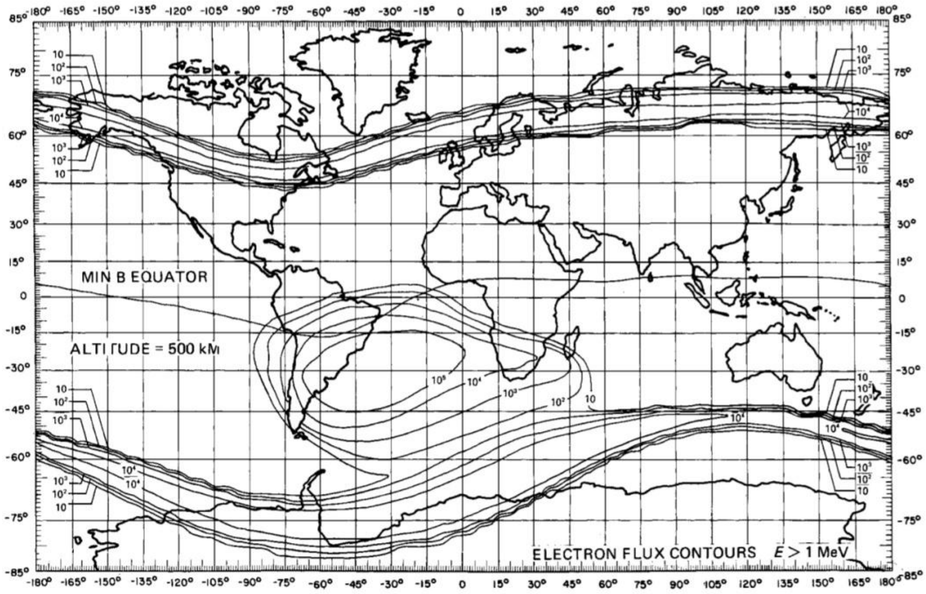

Figure 1: Omni-directional flux in electrons cm^{-2} s^{-1}. Credit: [3]

Figure 2 shows the flux of protons with energy $E > 30$ MeV with highest concentration in SAA.

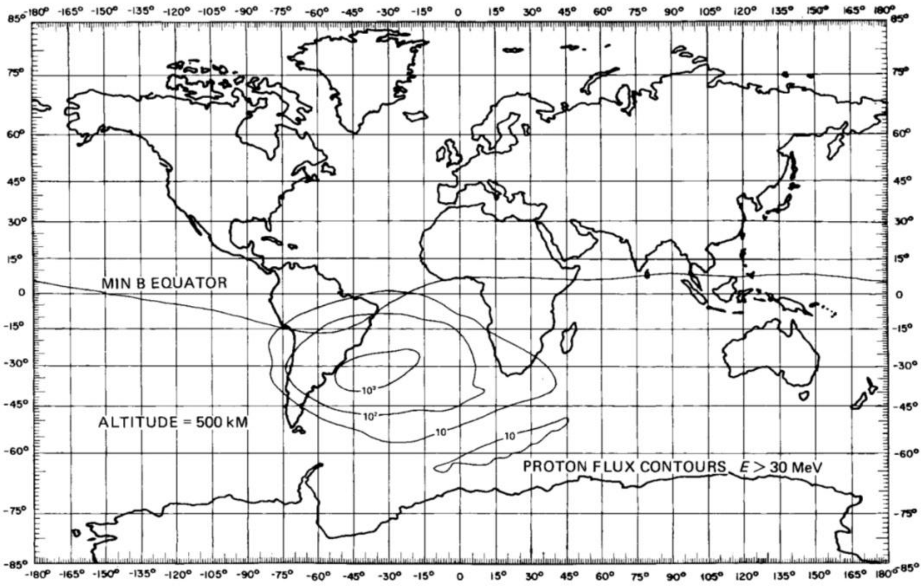

Figure 2: Omni-directional flux in protons cm^{-2} s^{-1}. Credit: [3]

If the low-Earth orbit of an instrument dedicated for GRB observations is chosen to have high inclination ($i \gtrsim 50°$), for example polar orbit, then one can expect high background count rate at polar regions caused by the trapped electrons in the outer and inner Van Allen radiation belts.

Figure 3 shows a map of electron fluxes with energies higher than 40 keV at the altitude 500 km as obtained from the European Space Agency's (ESA) SPace ENVironment Information System (SPENVIS)[1] developed by the Royal Belgian Institute for Space Aeronomy (BIRA-IASB). The map is based on the ESA-SEE1 model, which is an update of NASA's AE-8 model employing the CRRES/MEA satellite data from 1990-1991 [4, 5] for solar minimum.

[1] https://www.spenvis.oma.be

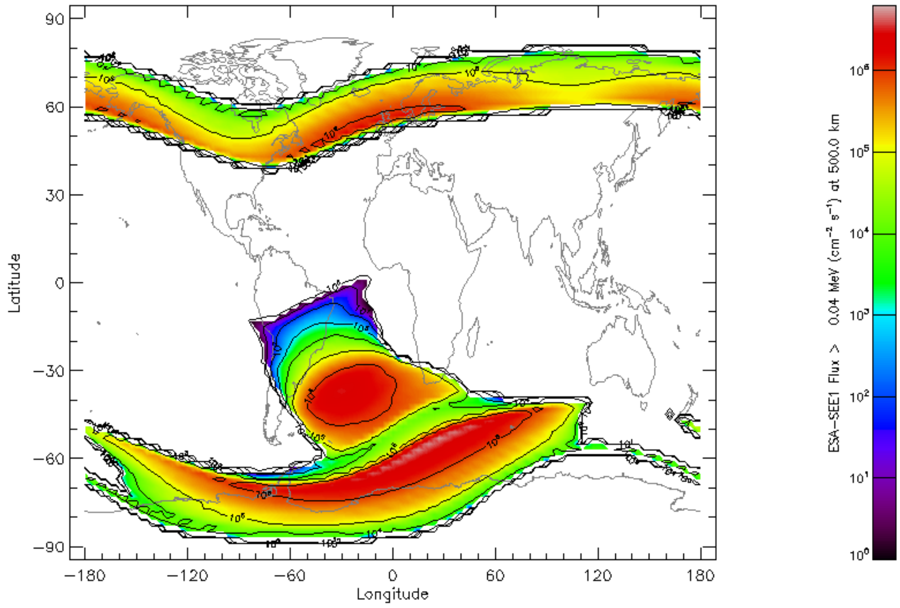

Figure 3: A map of electron fluxes with energies higher than 40 keV at the altitude 500 km based on the ESA-SEE1 model. Credit: SPENVIS and [4]

Figure 4 shows a map of proton fluxes with energies higher than 0.1 MeV at the same altitude (also obtained from SPENVIS). The map is based on NASA's AP-8 model [6] for solar minimum.

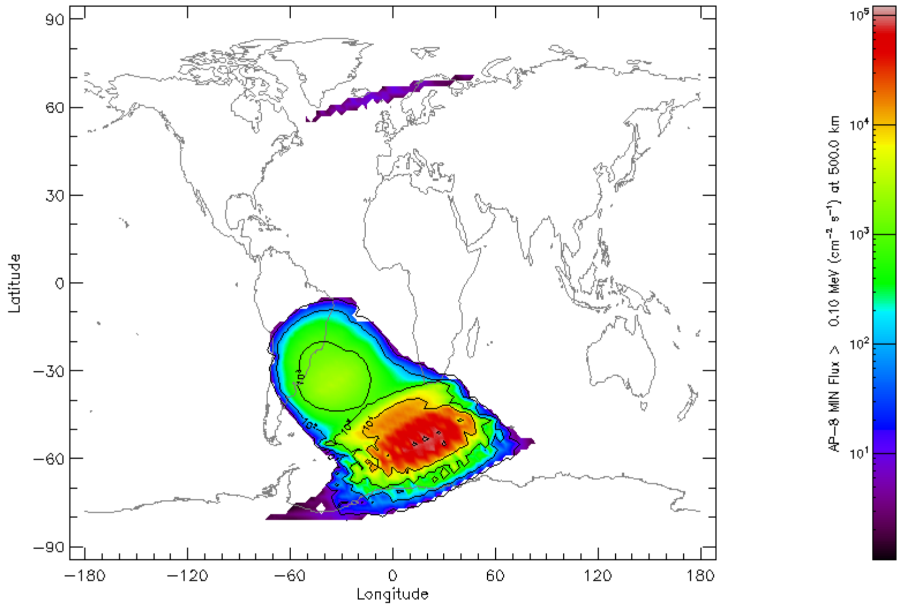

Figure 4: A map of proton fluxes with energies higher than 0.1 MeV at the altitude 500 km based on the AP-8 model. Credit: SPENVIS and [6]

Figure 5 shows a map of the radiation dose rate of charged particles (electrons and protons) at low-Earth orbit (LEO) as measured by the *Lomonosov*/Depron instrument. The *Lomonosov* satellite was launched to a low-Earth (altitude of ~480 km) sun-synchronous polar orbit (i = 97.2°) [10] with charged particle and gamma-ray detectors onboard. Therefore, the data collected by this mission provide a good reference for the expected background for any soft gamma-ray detector on high-inclination LEO.

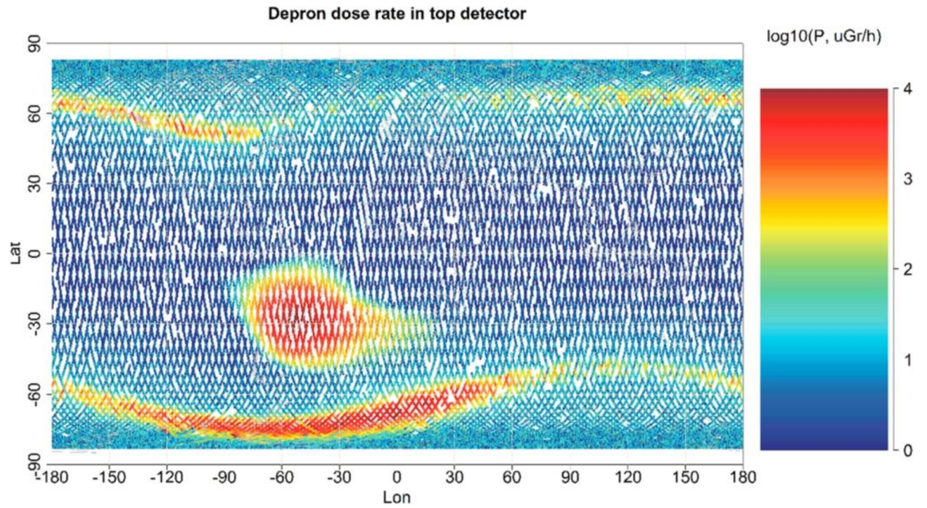

Figure 5: Map of the radiation environment for SSO as measured by the *Lomonosov*/DEPRON instrument. Credit: [7]

One of the instruments on board the *Lomonosov* satellite is the BDRG instrument, dedicated to detect GRBs. It consists of three modules with NaI(Tl) and CsI(Tl) scintillators read out by Hammamatsu R877 photomultiplier tubes (PMT). The scintillators are enclosed by a thin layer of aluminum and they are sensitive to gamma-rays from 10 keV to 3.0 MeV [9]. Figure 6, and Figure 7 show count rate variations in the *Lomonosov*/BDRG NaI(Tl) scintillator when crossing the polar regions.

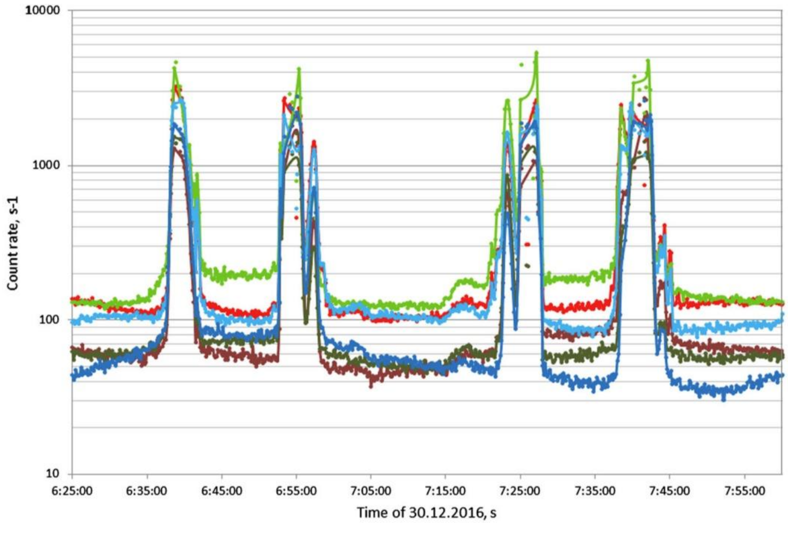

Figure 6: Count rate variations in the *Lomonosov*/BDRG NaI(Tl) scintillator on polar SSO: BDRG-1 20–35 keV (*light red line*), 6–10 keV (*dark red line*), BDRG-2 20–35 keV (*light green line*), 6–10 keV (*dark green line*), BDRG-3 20–35 keV (*light blue line*), 6–10 keV (*dark blue line*). Credit: [9]

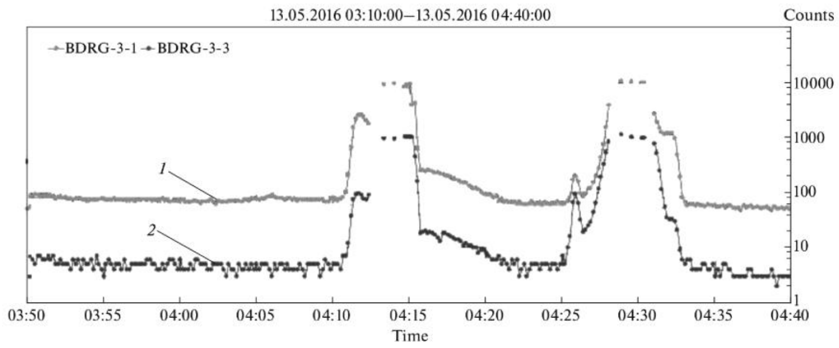

Figure 7: Count rates of the *Lomonosov*/BDRG instrument (BDRG-3 box, NaI(Tl)) when crossing the polar region in channels: (1) 30–50 keV; (2) 100–200 keV. Credit: [8]

According to the *Lomonosov*/BDRG observations, the count rate in the 10-450 keV energy range increases ~40 times in the polar regions compared to the equator. Such high background count rates, which last for about 1/3 of the duration of the polar orbit, make the detection of GRBs difficult. The fast background variations can also cause false triggers, which can be avoided by disabling the algorithm during the polar passes.

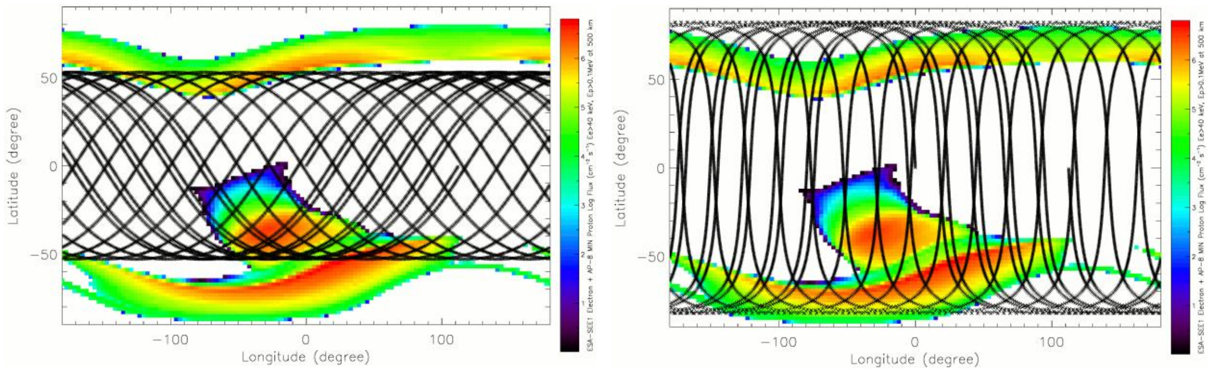

Figure 8: Displayed are 20 circular orbits out of 1000 simulated orbits at altitude of 500 km with inclination of 53° (left) and for polar orbit with inclination of 97.6° (right). The colour maps are the combined fluxes of trapped electrons (ESA-SEE1 model) and protons (AP-8) for solar minimum.

The *Lomonosov*/BDRG instrument gives us lesson that a scintillation detector at LEO will experience high particle background, respond to this high particle background and thus record high count rate. Therefore, we calculated an average fraction of the time during which a satellite will be in an area of high particle background. We simulated 1000 circular orbits at the altitude of 500 km and with inclination 53°and 97.6°, respectively (see Figure 29). Since the measurements of the *Lomonosov*/BDRG gamma-ray detector show that the count rate due to the electrons and protons increases rapidly, when the satellite enters the radiation belts and SAA, we calculated the average fraction of the time when the satellite is at a region with combined electron and proton flux > 1 $s^{-1}cm^{-2}$. We used the ESA-SEE1 model for the solar minimum for the electron flux obtained from SPENVIS. For the proton flux we used the AP-8 model for the solar minimum also obtained from SPENVIS.

Results show that if we place the constellation to SSO we will lose 32 % of observing time per satellite due to high background at polar region and during the passes through the SAA. If the constellation is launched to SSO then we will most likely require more than 9 satellites to compensate for the loss of observing time. In the case of the Walker orbits with an inclination of 53° the loss of observing time would be 23 % and it would affect only the observations near the edges of the polar regions and in the SAA.

[1] Zombeck M. V. 2007, *Handbook of Space Astronomy and Astrophysics*, Cambridge University Press, New York

[2] Walt M. 1994, *Introduction to Geomagnetically Trapped Radiation*, Cambridge Atmospheric and Space Science Series, Cambridge University Press, New York

[3] Stassinopoulos E. G. 1970, *World Maps of Constant B, L, and Flux Contours*, NASA SP-3054

[4] Vampola, A. L. 1996, *Outer Zone Energetic Electron Environment Update*, Final Report of ESA/ESTEC Contract No.

[5] Vette J. I. 1991, *The AE-8 Trapped Electron Model Environment*, NSSDC/WDC-A-R&S 91-24

[6] Sawyer D. M., and Vette J. I. 1976, *AP-8 Trapped Proton Environment for Solar Maximum and Solar Minimum*, NSSDC/WDC-AR&S 76-06

[7] Benghin V. V., Nechaev O. Y., Zolotarev I. A., et al. 2018, Space Science Review, 214, 9

[8] Panasyuk M. I., Lipunov V. M., Park I., et al. 2018, Physics of Particles and Nuclei, 49, 109

[9] Svertilov S. I., Panasyuk M. I., Bogomolov V. V., et al. 2018, Space Science Reviews, 214, 8

[10] Sadovnichii V. A., Panasyuk M. I., Amelyushkin A. M., et al. 2017, Space Science Reviews, 212, 1705